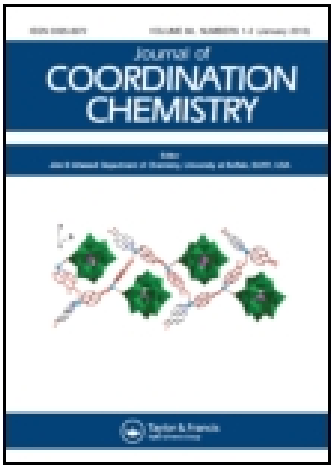

Journal of Coordination Chemistry
Publication details, including instructions for authors and subscription information:
http://www.tandfonline.com/loi/gcoo20

Synthesis and X-ray crystal structures of three new terpyridine-based Pb(II) complexes, cytotoxicity studies of $\{[Pb(ttpy)(\mu\text{-}AcO)]_2\}(SCN)_2$

Lotfali Saghatforoush[a], Ertan Sahin[b], Somayyeh Babaei[a], Akbar Bakhtiari[a], Ahmad Nasimian[c], Ömer Çelik[d] & Zohreh Zabihollahi[a]

[a] Department of Chemistry, Payame Noor University, Tehran, Iran

[b] Faculty of Science, Department of Chemistry, Atatürk University, Erzurum, Turkey

[c] Department of Clinical Chemistry, Tehran University of Medical Sciences, Tehran, Iran

[d] Faculty of Education, Fizik Department, Dicle University, Diyarbakır, Turkey

Accepted author version posted online: 31 Mar 2014.Published online: 06 May 2014.

To cite this article: Lotfali Saghatforoush, Ertan Sahin, Somayyeh Babaei, Akbar Bakhtiari, Ahmad Nasimian, Ömer Çelik & Zohreh Zabihollahi (2014) Synthesis and X-ray crystal structures of three new terpyridine-based Pb(II) complexes, cytotoxicity studies of $\{[Pb(ttpy)(\mu\text{-}AcO)]_2\}(SCN)_2$, Journal of Coordination Chemistry, 67:8, 1463-1477, DOI: 10.1080/00958972.2014.909930

To link to this article: http://dx.doi.org/10.1080/00958972.2014.909930

Journal of Coordination Chemistry, 2014
Vol. 67, No. 8, 1463–1477, http://dx.doi.org/10.1080/00958972.2014.909930

Synthesis and X-ray crystal structures of three new terpyridine-based Pb(II) complexes, cytotoxicity studies of $\{[Pb(ttpy)(\mu\text{-}AcO)]_2\}(SCN)_2$

LOTFALI SAGHATFOROUSH*†, ERTAN SAHIN‡, SOMAYYEH BABAEI†, AKBAR BAKHTIARI†, AHMAD NASIMIAN§, ÖMER ÇELIK¶ and ZOHREH ZABIHOLLAHI†

†Department of Chemistry, Payame Noor University, Tehran, Iran
‡Faculty of Science, Department of Chemistry, Atatürk University, Erzurum, Turkey
§Department of Clinical Chemistry, Tehran University of Medical Sciences, Tehran, Iran
¶Faculty of Education, Fizik Department, Dicle University, Diyarbakır, Turkey

(*Received 29 September 2013; accepted 11 March 2014*)

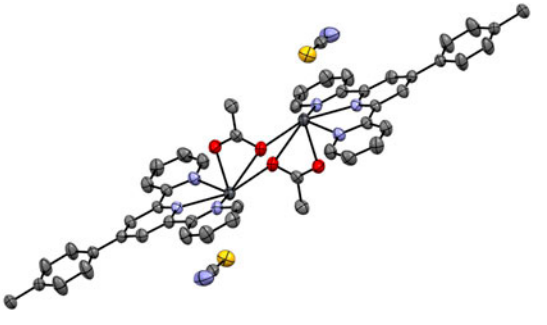

Synthesis and X-ray crystal structures of three new terpyridine-based Pb(II) complexes, $\{[Pb(ttpy)(\mu\text{-}AcO)]_2\}(SCN)_2$ (**1**) (ttpy = 4′-tolyl-2,2′:6′,2″-terpyridine), $[Pb(Clphtpy)(AcO)(ClO_4)]$ (**2**), and $[Pb(Clphtpy)(SCN)_2]$ (**3**) (Clphtpy = 4′-(4-chlorophenyl)-2,2′:6′,2″-terpyridine), are described. The synthesized materials have been characterized, also, by CHN elemental analysis, ^{1}H NMR, and IR spectroscopy. The structural analyses showed that, in the solid state, the coordination number of Pb(II) in **1**, **2**, and **3** are six, seven, and five, respectively. In the complexes, the lone-pair electrons of Pb(II) are stereochemically active and the coordination geometry of Pb(II) is hemidirected. The structures of the three complexes were compared and the effect of counter ion is described. The antibacterial activity of **1** and previously reported $\{[Pb(ttpy)(\mu\text{-}AcO)]_2\}(PF_6)_2$ (**1A**) and $\{[Pb(ttpy)(\mu\text{-}AcO)I]_2\}$ (**1B**) were tested by minimum inhibitory concentration method to investigate the effect of counter ions on biological activity of the compounds. Also, cytotoxicity test was assessed using 3-[4,5-dimethylthiazol-2-yl]-2,5 diphenyl tetrazolium bromide assay to determine the maximum non-toxic concentration of ttpy, Pb(II), and their complexes to HepG2 cells. Effective lead detoxification was observed for **1**, **1A**, and **1B**.

Keywords: Lead(II) complex; Terpyridine; X-ray crystal structure; Antibacterial activity; Cytotoxicity; Lead poison detoxification

*Corresponding author. Emails: l_saghatf@pnu.ac.ir, saghatforoush@gmail.com

1. Introduction

Inner and outer-sphere coordination of metal complexes are of interest in inorganic chemistry. The inner-sphere coordination has great influence on the complex chemistry and the outer-sphere coordination can affect the inner-sphere characteristics such as bond lengths and angles [1]. Development of more sensitive spectroscopic techniques and availability of a variety of solid-state structures of similar complexes made the study of these effects easier [2]. Interesting properties of lead(II) complexes [3], despite toxicological effects of Pb(II), made Pb(II) an attractive species to study: (1) It has a $6s^2$ outer electron configuration and a large radius, which can lead to interesting topological arrangements [4]. This allows Pb^{2+} to coordinate as holodirected, where the ligand donors are directed throughout the surface of encompassing sphere, or as hemidirected, where the ligand donors are directed throughout only part of coordination sphere leaving a gap in the distribution of bonds to ligands [5]. (2) The absence of crystal field stabilization energy affects Pb^{2+} to adopt various coordination geometries including octahedral, tetrahedral, or square planar [6, 7]. (3) Many complexes possess bioactivity and several drugs have been developed based on metal complexes [8, 9]. Chelating agents can be designed to remove lead compounds after ingestion in the human body [10]. In the design of drugs to counteract the effects of lead poisoning, it is necessary to establish the preferred ligands of lead and their stereochemistry and to compare these with the requirements of other essential metal ions such as zinc [11]. (4) Ability to bind well to both hard and soft donors [12].

Due to their promising applications in drug chemistry and materials chemistry, coordination chemistry, and crystal structures of metal complexes of 2,2′:6′,2″-terpyridine (tpy) have been well studied [13–20]. Following our previous reports on metal complexes of 2,2′:6′,2″-terpyridine (tpy)-based ligands [20(a)–(f)], here we report the synthesis of three new complexes, $\{[Pb(ttpy)(\mu\text{-}AcO)]_2\}(SCN)_2$ (**1**) (ttpy = 4′-tolyl-2,2′:6′,2″-terpyridine), [Pb(Clphtpy)(AcO)(ClO_4)] (**2**), and $[Pb(Clphtpy)(SCN)_2]$ (**3**) (Clphtpy = 4′-(4-chlorophenyl)-2,2′:6′,2″-terpyridine). Coordination sphere of Pb(II) and ligand coordination modes in the complexes are described in the solid-state based on X-ray crystal structure data. The crystal structures are compared with previously reported similar lead complexes and the effect of the counter ions on the crystal structures is discussed. Moreover, the effects of counter anions and activity of the electron lone pair on lead(II) on cytotoxicity and antibacterial activity of **1** and previously reported $\{[Pb(ttpy)(\mu\text{-}AcO)]_2\}(PF_6)_2$ (**1A**) and $\{[Pb(ttpy)(\mu\text{-}AcO)I]_2\}$ (**1B**) [20(f)] are investigated by 3-[4,5-dimethylthiazol-2-yl]-2,5 diphenyl tetrazolium bromide (MTT) and minimum inhibitory concentration (MIC) assays, respectively.

2. Experimental

2.1. *Materials and measurements*

All reagents were used as supplied by Merck and Aldrich without purification. Syntheses of $\{[Pb(ttpy)(\mu\text{-}AcO)]_2\}(PF_6)_2$ (**1A**) and $\{[Pb(ttpy)(\mu\text{-}AcO)I]_2\}$ (**1B**) were reported previously by our group [20(f)]. ^{1}H NMR spectra were measured with a BRUKER 400 Ultra-Shield spectrometer at 400 MHz and all chemical shifts are reported in δ units downfield from Me_4Si. FT-IR spectra were collected on a Shimadzu-IR Prestige 21 spectrophotometer from 4000 to 400 cm^{-1} using KBr pellets. Elemental analyses were carried out using a Heraeus CHN–Rapid analyzer. Melting points were measured on an electrothermal 9100 apparatus.

2.2. *Synthesis of {[Pb(ttpy)(μ-AcO)]$_2$}(SCN)$_2$ (1)*

The complex was synthesized in the same way as previously reported for similar lead(II) complexes [20(f)] using the arm-branched tube method, under thermal gradient: ttpy (1 mM, 0.323 g), potassium thiocyanate (2 mM, 0.194 g), and lead(II) acetate (1 mM, 0.360 g) were placed in the main arm of a branched tube. Methanol was carefully added to fill both arms, then the tube was sealed and the main arm was immersed in a bath at 60 °C, while the other remained at ambient temperature. After 15 days, light brown crystals were deposited in the cooler arm, filtered off, washed with acetone, and air-dried (1.018 g, yield 88%), m.p. 230 °C. Anal. Calcd for $C_{25}H_{20}N_4O_2SPb$: C, 46.35; H, 3.11; N, 8.64. Found (%): C, 46.31; H, 3.14; N, 8.66. IR (KBr) (ν_{max}, cm^{-1}): 3063.12 (C–H, arom); 2920.30 (C–H, aliph); 1399.81–1600.08 (C=C, arom); 1393.33 [ν_{sym}(COO)] and 1570.78 [ν_{as}(COO)]; 1544.13 (C=N, Py); 2097.77 (C=N, SCN); 787.07 (C=S, SCN). ^{1}H NMR (DMSO-d_6) δ_H: 1.69 (3H, s, $CH_{3\text{-phenyl}}$); 2.41 (3H, s, CH_3); 7.42 (2H, d, arom); 7.61 (2H, t, arom); 7.93 (2H, d, arom); 8.11 (2H, t, arom); 8.72 (2H, d, arom); 8.76 (2H, s, arom); 8.83 (2H, d, arom).

2.3. *Synthesis of [Pb(Clphtpy)(AcO)(ClO$_4$)] (2)*

The complex was synthesized in the same way as **1** using Clphtpy instead of ttpy and sodium perchlorate instead of potassium thiocyanate. After 4 days, light yellow crystals were deposited in the cooler arm, filtered off, washed with acetone, and air-dried (yield 59%), m.p. 347 °C (dec.). Anal. Calcd for $C_{23}H_{16}Cl_2N_3O_6Pb$: C, 38.98; H, 2.28; N, 5.96. Found (%): C, 39.15; H, 2.09; N, 5.77. IR (KBr) (ν_{max}, cm^{-1}): 3082 (C–H, arom); 2906 (C–H, aliph); 1406.11–1610.56 (C=C, arom); 1388.75 [ν_{sym}(COO)] and 1543.05 [ν_{as}(COO)]; 1543.13 (C=N, Py); ^{1}H NMR (DMSO-d_6) δ_H: 3.36 (3H, s, CH_3); 7.65–7.69 (4H, t, arom); 8.09 (2H, d, arom); 8.15 (2H, t, arom); 8.76 (2H, d, arom); 8.80 (2H, s, arom); 8.89 (2H, bs, arom).

2.4. *Synthesis of [Pb(Clphtpy)(SCN)$_2$] (3)*

The complex was synthesized in the same way as **2** using potassium thiocyanate instead of sodium perchlorate. After 7 days, yellow crystals deposited in the cooler arm were filtered off, washed with acetone, and air-dried (yield 67%), m.p. 292 °C (dec.). Anal. Calcd for $C_{23}H_{14}ClN_5S_2Pb$: C, 41.68; H, 2.39; N, 10.18. Found (%): C, 41.40; H, 2.11; N, 10.05. IR (KBr) (ν_{max}, cm^{-1}): 3055 (C–H, arom); 1415.15–1604.77 (C=C, arom); 2071.45 and 2052.37 (C=N, SCN); 780.62 (C=S, SCN), 1519.37 (C=N, Py); ^{1}H NMR (DMSO-d_6) 7.65–7.71 (4H, t, arom); 8.10 (2H, d, arom); 8.15 (2H, t, arom); 8.75 (2H, d, arom); 8.80 (2H, s, arom); 8.95 (2H, bs, arom).

2.5. *X-ray crystallography*

For the crystal structure determination, single crystals of **1–3** were used for data collection on a four-circle Rigaku R-AXIS RAPID-S diffractometer (equipped with a 2-D area IP detector). Graphite-monochromated Mo Kα radiation ($\lambda = 0.71073$ Å) and oscillation scans technique with $\Delta\omega = 5°$ for one image were used for data collection. The lattice parameters were determined by the least-squares methods on the basis of all reflections with

$F^2 > 2\sigma(F^2)$). Integration of the intensities, correction for Lorentz, and polarization effects and cell refinement were performed using crystal clear (Rigaku/MSC Inc., 2005) software [21]. The structures were solved by direct methods using SHELXS-97 and refined by full-matrix least-squares using SHELXL-97 [22]. All non-hydrogen atoms were refined anisotropically. Hydrogens were positioned geometrically and refined using a riding model. The final difference Fourier maps showed no peaks of chemical significance. A summary of crystal data and refinement results are provided in table 1.

2.6. *Biological methods*

2.6.1. Antibacterial activity. *Streptococcus pyogenes* (Gram-positive bacterium) and *Klebsiella pneumonia* and *Escherichia coli* (Gram-negative bacteria) were used to test the activity of ttpy, lead(II), **1**, **1A**, and **1B**. Antibacterial activities have been assayed using the MIC method proposed by Malik [23]. Bacteria were inoculated into 5 mL of liquid SCD (soybean, casein, and digest) medium and cultured for 24 h at 35.5 °C. The cultured fluids were diluted, adjusted to 10^5–10^6 micro-organisms per mL and used for inoculation in the MIC test. Test compounds were suspended in water and then diluted with SCD medium for bacteria. Then twofold diluted solutions with concentrations of 20–2000 μg mL^{-1} were prepared. Each 1 mL of culture medium was inoculated with 0.1 mL of the micro-organism

Table 1. Crystallographic data of **1**, **2**, and **3**.

Identification code	Complex **1**	Complex **2**	Complex **3**
Empirical formula	$C_{25}H_{20}N_4O_2PbS$	$C_{23}H_{16}Cl_2N_3O_6Pb$	$C_{23}H_{12}ClN_5S_2Pb$
Formula weight	647.7	709.49	665.14
Temperature (K)	293(2)	293(2)	293(2)
Wavelength (Å)	0.71073	0.71073	0.71073
Crystal system	Triclinic	Monoclinic	Monoclinic
Space group	*P-1*	$P2_1/n$	*C2/c*
Unit cell dimensions (Å, °)	$a = 8.8705$ (2)	$a = 15.6240$ (7)	$a = 17.6628$ (9)
	$b = 9.9170$ (3)	$b = 9.2175$ (5)	$b = 18.2375$ (10)
	$c = 14.1006$ (5)	$c = 15.8397$ (6)	$c = 7.5145$ (5)
	$\alpha = 76.994$ (3)°	$\alpha = 90°$	$\alpha = 90°$
	$\beta = 83.479$ (2)°	$\beta = 103.474$ (3)°	$\beta = 113.8906$ (26)°
	$\gamma = 72.149$ (2)°	$\gamma = 90°$	$\gamma = 90°$
Volume (Å^3)	1149.08 (6)	2218.35 (18)	2213.2 (2)
Z	2	4	4
Density (Calcd) (g cm^{-3})	1.872	2.124	1.996
Absorption coefficient (mm^{-1})	7.463	7.895	7.954
F (0 0 0)	624	1360	1264
θ Range for data collection (°)	2.4–26.4	2.09–30.65	2.23–30.53
Index ranges	$-11 \le h \le 11$	$-22 \le h \le 22$	$-25 \le h \le 25$
	$-12 \le k \le 12$	$-13 \le k \le 12$	$-23 \le k \le 25$
	$-16 \le l \le 17$	$-19 \le l \le 22$	$-9 \le l \le 10$
Reflections collected	24,840	21,135	9797
Data/restraints/parameters	4683/0/301	6753/6/320	3380/0/149
Goodness-of-fit on F^2	1.082	1.065 (restrained S:1.085)	1.023
Final *R* indices [$I > 2\sigma(I)$]	$R_1 = 0.0428$	$R_1 = 0.0916$	$R_1 = 0.0513$
	$wR_2 = 0.0867$	$wR_2 = 0.214$	$wR_2 = 0.0944$
R indices (all data)	$R_1 = 0.0564$	$R_1 = 0.1821$	$R_1 = 0.0987$
	$wR_2 = 0.0977$	$wR_2 = 0.2398$	$wR_2 = 0.1177$
Largest diff. peak, hole (e Å^{-3})	2.225 and −0.918	3.006 and −2.253	2.102 and −0.982

suspension prepared as described above. Then, bacteria were cultured for 24 h at 35.5 °C. Growth of the micro-organisms was monitored during this period. MIC of the test material was defined as the lowest concentration of test materials for which no growth of micro-organism was observed in the medium. Gentamicin was used as standard control, treated as the other tested compounds.

2.6.2. Cytotoxicity assay. HepG2 cells were maintained in RPMI 1640 medium. All media were supplemented with newborn calf serum (10%). Cultures were incubated at 37 °C in a humidified atmosphere of 5% CO_2 : 95% air. All cultures were daily passaged. Assays of cytotoxicity were conducted in 96-well, flat-bottomed microtitre plates. The supplemented culture medium (50 µL) with cells (1×10^5 cells mL^{-1}) was added to the wells. The test compounds were dissolved in DMSO and diluted in the culture medium with final concentrations of 2–2000 µg mL^{-1}. Fifty microliters of the prepared solutions were added to each well. The microtitre plates were incubated at 37 °C in a humidified atmosphere of 5% CO_2 : 95% air for 48 h. All the assays were run in parallel with a negative and a positive control, in which cisplatin was used as cytotoxic agent. The evaluation of cytotoxicity was carried out using a modified method of MTT assay. About 10 µL of MTT solution with a concentration of 4 mg mL^{-1} was added into each well. After 2 h incubation at 37 °C in a humidified atmosphere of 5% CO_2 : 95% air, a water solution containing 10% w : v of SDS and 50% v : v of DMF was added into each well to lyse the cells and to solubilize the formed formazan complex. After 20 h incubation, the OD value was measured using a microtitre plate reader at 570 nm and the percentages of cell survival were determined. The cytotoxicity was evaluated based on the percentage cell survival in a dose-dependent manner relative to the negative control.

3. Results and discussion

3.1. *Spectroscopy*

Reaction of lead(II) acetate with tpy derivatives in the presence of potassium thiocyanate and sodium perchlorate in methanol yielded crystalline **1–3**. IR spectra of all complexes show absorptions resulting from skeletal vibrations of aromatic rings at 1399–1610 cm^{-1} [24]. The relative weak absorption bands at 3055–3082 cm^{-1} and 2906–2920 cm^{-1} are due to aromatic and aliphatic C–H stretches, respectively. Bands at 1388 and 1393 cm^{-1} in the IR spectrum of **1** and those observed at 1543 and 1573 cm^{-1} in the IR spectrum of **2** are assigned, respectively, to ν_{as} and ν_s of acetate. In **1**, ν(CN) and ν(CS) of thiocyanate were observed at 2097 and 787 cm^{-1}, respectively. In comparison, the ν(CN) and ν(CS) vibration modes for coordinated thiocyanate were observed at 2076–2052 cm^{-1} and 780 cm^{-1}, respectively, in the IR spectrum of **3**. The intense and broad band at 1087 cm^{-1} is assigned to perchlorate in the IR spectrum of **2**. The ^{1}H NMR spectra of the DMSO solutions of all complexes display expected resonances assigned to aromatic C–H protons of ttpy or Clphtpy. Corresponding singlet resonances of aliphatic C–H protons were observed at 1.69, 2.41 for **1** and at 3.36 ppm for **2**.

3.2. *Crystal structure of 1*

Complex **1** crystallizes in the triclinic system (space group *P-1*). Figure 1 shows the molecular structure and crystal packing and some selected bond distances and angles are listed in table 2. Also, the hydrogen bonding parameters and weak interaction distances are given in table 3. In the solid state, comparable with previously reported $\{[Pb(ttpy)(\mu\text{-}AcO)]_2\}(PF_6)_2$ (**1A**) [20(f)], the crystal structure consists of $\{[Pb(ttpy)(AcO)]_2\}^{2+}$ dimerized cationic units neutralized by two thiocyanates. Similar to **1A** and $\{[Pb(ttpy)(\mu\text{-}AcO)I]_2\}$ (**1B**) [20(f)], each lead is chelated by three ttpy nitrogens. Also, three oxygens from two acetates are coordinated to each lead (table 2). As shown in figure 1(a), one oxygen from each acetate forms a bridge between two lead ions to produce dimeric units in the solid state. A highly distorted six-coordinate geometry is observed for lead(II) in **1**. The corresponding Pb…Pb distance

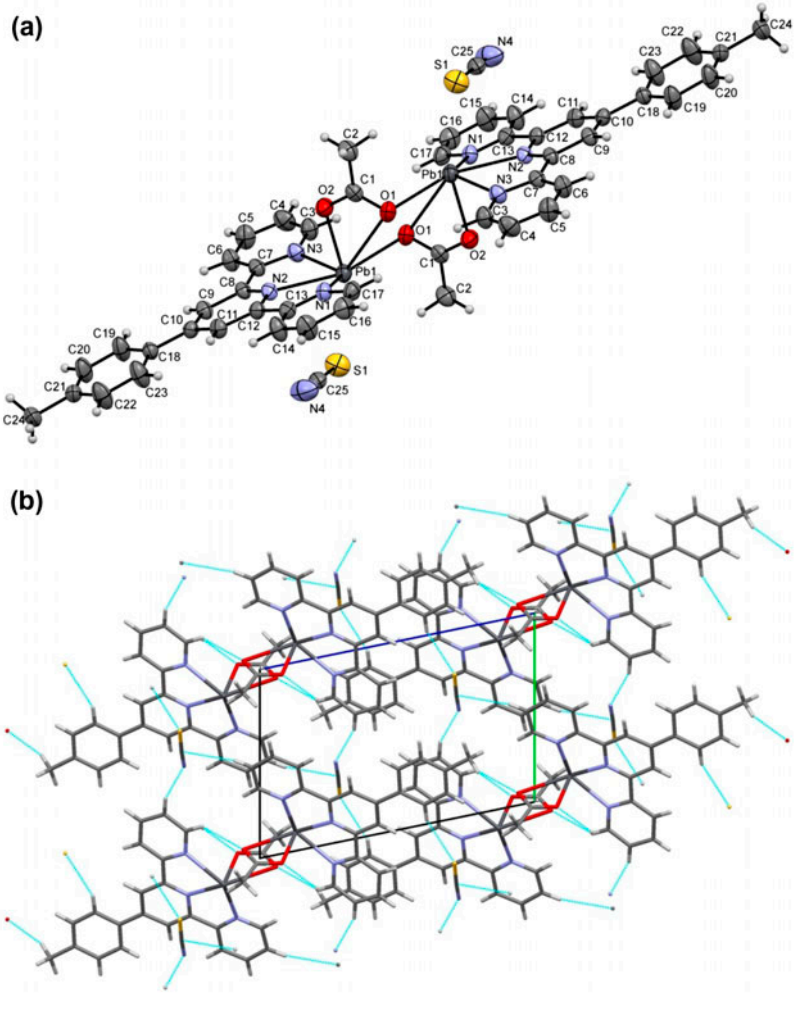

Figure 1. (a) ORTEP view of **1** with the atom numbering scheme. Displacement ellipsoids are shown at the 30% probability level. (b) Packing diagram of **1**. Hydrogen bonds are indicated by dashed lines.

Table 2. Selected bond distances (Å) and angles (°).

Complex **1**		Complex **2**		Complex **3**	
N1–Pb1	2.591(6)	N1–Pb	2.648 (14)	N2–Pb	2.466(6)
N2–Pb1	2.482(5)	N2–Pb	2.505(12)	N3–Pb	2.494(7)
N3–Pb1	2.484(6)	N3–Pb	2.550(13)	S1–Pb	2.951(3)
O2–Pb1	2.302(5)	O2–Pb	2.80(2)		
O1–Pb1	2.862(6)	O1–Pb	2.530(11)		
O1a–Pb1	2.937(7)	O3–Pb	3.01(1)		
		O5–Pb	3.07(1)		
N1–Pb1–N2	64.64(17)	N1–Pb–N2	65.3(4)	N2–Pb–N3	64.99(12)
N2–Pb1–N3	65.36(18)	N2–Pb–N3	64.4(4)	N2 Pb N2	130.0(2)
N1–Pb1–N3	127.68(19)	N1–Pb–N3	128.2(4)	S1–Pb–S1a	164.39(10)
N1–Pb1–O1	77.8(2)	N1–Pb–O1	86.6(4)	N2–Pb–S1	87.17(15)
O1–Pb1–O2	49.1(2)	O1–Pb–O2	47.1(4)	N2–Pb–S1a	86.25(14)
O2–Pb1–N2	85.25(18)	N1–Pb–O2	72.3(5)	N3–Pb–S1	82.20(5)
O1–Pb1–N3	120.5(2)	N3–Pb–O1	77.2(4)	N3–Pb–S1a	82.20(5)
O1–Pb1–N2	124.3(2)	N3–Pb–O2	121.6(5)		
O2–Pb1–N1	82.79(19)	N2–Pb–O1	84.5(4)		
O2–Pb1–N3	78.77(19)	N2–Pb–O2	116.4(5)		
O1–Pb1–O1a	71.7(2)	O5–Pb–O3	44.4(3)		
Pb1–O1–Pb1a	108.3(2)	O5–Pb–N1	68.2(4)		
		O5–Pb–N2	67.5(4)		
		O3–Pb–N3	69.6(4)		
		O3–Pb–N2	79.1(4)		

in the described cationic dimers is 4.7024(5) Å. For **1A**, a comparable value of 4.741(2) Å was previously reported for Pb…Pb distance. In contrast, the discussed distance is slightly shorter for **1B** (4.5969(4) Å) possibly due to a different coordination sphere of the metal centers, compared with that of **1**.

The Pb–N(2) bonds to the central pyridine in **1** (bond distance of 2.482(5) Å) are comparable with those found for **1A** (2.506(2) Å) and **1B** (2.491(6) Å) [20(f)]. The Pb–N bonds to the side pyridine groups in ttpy are 2.484(6) and 2.591(6) Å (compared to the 2.532(2) and 2.612(2) Å in **1A** and 2.515(5) and 2.558(7) Å in **1B** [20(f)]). The non-bridging Pb–O(2) bond distances are 2.302(5) Å in **1**. In comparison, the non-bridging Pb–O bond lengths in **1A** and **1B** are 2.297(2) and 2.353(5) Å, respectively [20(f)]. The bridging Pb–O(1) and Pb–O(1a) distances in **1** are rather long (2.862(6) and 2.937(7) Å, respectively). Also, long-bridging Pb–O bonds are observed for **1A** (2.813(3) and 2.957(3) Å) and **1B** (2.890(6) and 2.948(1) Å) [20(f)]. These long-bridging Pb–O bonds point towards the presence of a sterically active electron lone pair on lead. This is supported by shortening of the Pb–N(2) and non-bridging Pb–O(2) bonds on the side of the Pb(II) ion, opposite to the putative lone pair of electrons.

The N–Pb–N angles in the five-membered chelate rings are 64.64(17)° and 65.36(18)°. Also, the N(1)–Pb–N(3) angle is 127.68(19)°. The angles formed by non-bridging oxygen, positioned in the basal coordination site, are O(2)–Pb(1)–N(2) (85.25(18)°), O(2)–Pb(1)–N(3) (78.77(19)°), O(2)–Pb(1)–N(1) (82.79(19)°), O(2)–Pb(1)–O(1) (49.1(2)°) and O(2)–Pb(1)–O (1a) (88.4(2)°). With the bridging oxygens, the O(1)–Pb(1)–O(1a) angle is 71.7(2)°, compared to 69.45(9)° in **1A** and 76.1(2)° in **1B** [20(f)]. Moreover, the Pb(1)–O(1)–Pb(1a) angle (108.3 (2)°) is close to the corresponding value observed in **1A** (110.6(1)°), however, larger than that that in **1B** (103.9(2)°) [20(f)].

Table 3. Hydrogen bonds and intermolecular interactions (contact length of longer than the sum of covalent radii and shorter than the sum of vdW radii) (Å and °) for **1–3**.

D–H···*A*	*D*–H (Å)	*H*···*A*	*D*···*A* (Å)	∠*D*–H···*A* (°)	Symmetry code
Complex **1**					
C(3)–H(3)···O(1)	0.93	2.541	3.30(1)	138.8	$-x, -y, -z$
C(24)–H(24C)···O(2)	0.96	2.452	3.37(1)	160.4	$1-x, -y, 1-z$
C(4)–H(4)···N(4)	0.93	2.42	3.30(2)	158.6	$-x, -y, 1-z$
C(19)–H(19)···S(1)	0.93	2.783	3.65(1)	156.1	$x, 1+y, z$
C(16)–H(16)···C(25)	0.93	2.762	3.66(1)	161.4	$x, y, -1+z$
Weak interactions					
Pb···S(1)		3.429(3)			$-x, 1-y, 1-z$
Pb···C(25)		3.570(9)			$-x, 1-y, 1-z$
Pb···C(1)		3.536(9)			$-x, -y, -z$
N(4)···C(12)		3.11(1)			$-x, 1-y, 1-z$
Complex **2**					
C(4)–H(4)···O(6)	0.93	2.55	3.17(3)	125	$-x, 2-y, 2-z$
C(14)–H(14)···O(3)	0.8(1)	2.6(1)	3.37(2)	168(10)	$-x, 2-y, 1-z$
C(17)–H(17)···O(5)	0.93	2.49	3.28(2)	144	$-x, 2-y, 2-z$
C(21)–H(21)···O(6)	0.93	2.58	3.22(3)	126	$-1/2-x, -1/2+y, 1.5-z$
C(23)–H(23B)···O(5)	0.96	2.50	3.37(2)	151	$1/2-x, -1/2+y, 1.5-z$
C(3)–H(3)···O(6)	0.93	2.69	3.23(3)	118	$-x, 2-y, 2-z$
C(3)–H(3)···O(4)	0.93	2.61	3.24(3)	126	$1/2+x, 2.5-y, 1/2+z$
C(18)–H(18)···C(22)	0.93	2.83	3.64(3)	146	$-1/2+x, 1.5-y, 1/2+z$
C(14)–H(14)···C(23)	0.8(1)	2.88(9)	3.30(2)	114(9)	$-1/2+x, 1.5-y, -1/2+z$
C(23)–H(23A)···C(12)	0.96	2.52	3.46(2)	166	$1/2-x, 1/2+y, 1.5-z$
C(23)–H(23C)···C(14)	0.96	2.66	3.30(2)	125	$1/2+x, 1.5-y, 1/2+z$
C(23)–H(23C)···Cl	0.96	2.898	3.67(2)	138.6	$-x, 1-y, 2-z$
C(23)–H(23B)···Cl(2)	0.96	2.897	3.51(2)	122.6	$1/2-x, -1/2+y, 1.5-z$
Weak interactions					
C(23)–H(23B)···Pb	0.96	2.6404	2.97(2)	100.7	$1/2-x, -1/2+y, 1.5-z$
C(23)–H(23C)···Pb	0.96	2.5182	2.97(2)	108.9	$1/2-x, -1/2+y, 1.5-z$
Pb···O(1)		3.32(1)			$1/2-x, 1/2+y, 1.5-z$
Pb···C(22)		3.67(2)			$1/2-x, 1/2+y, 1.5-z$
Pb···Cl		3.544(5)			$1/2+x, 1.5-y, -1/2+z$
Pb···Cl(2)		3.616(5)			x, y, z
C(13)···Cl		3.37(2)			$-1/2-x, 1/2+y, 1.5-z$
C(23)···O(3)		3.18(2)			$1/2-x, -1/2+y, 1.5-z$
C(11)···O(2)		3.14(2)			$1/2-x, -1/2+y, 1.5-z$
C(6)···O(5)		3.17(2)			x, y, z
O(1)···O(2)		3.00(2)			$1/2-x, -1/2+y, 1.5-z$
Complex **3**					
C(12)–H(12)···N(1)	0.93	2.65	3.41(1)	139.2	$1.5-x, 1/2+y, 1/2-z$
C(5)–H(5)···N(1)	0.93	2.404	3.32(1)	167.0	$1.5-x, 1/2-y, 1-z$
C(3)–H(3)···C(12)	0.93	2.833	3.668(9)	150	$1.5-x, -1/2+y, 1.5-z$
C(5)–H(5)···C(1)	0.93	2.822	3.61(1)	143.3	$1.5-x, 1/2-y, 1-z$
Weak interactions					
S1···S2		3.524(3)			$1-x, y, -1/2-z$

In the oxygen bridged dimer cation, each Pb(II) has intramolecular weak interaction (contact length of longer than the sum of covalent radii and shorter than the sum of vdW radii) with the carboxylate carbon from the adjacent monomer. The corresponding Pb(1)…C(1a), N(1)-Pb(1)…C(1a) weak interaction length and angle are, respectively, 3.536(9) Å and 133.1(2)°. In the crystal packing, each Pb(II) is also connected, by weak interactions, to the sulfur (Pb(1)…S(1) length of 3.429(3) Å) and carbon (Pb(1)…C(25) length of 3.570(9) Å) from the thiocyanate counter ion in the vicinity. The S(1)…Pb(1)–N(1), S(1)…Pb(1)–N(2),

S(1)…Pb(1)–O(1), and S(1)…Pb(1)–O(1a) weak interaction angles are 105.2(1)°, 79.5(1)°, 152.7(1)°, and 95.5(1)°, respectively. The lead(II)-bonding mode in **1**, similar to **1A** and **1B**, could be described as hemidirected considering the coordination bonds and weak interactions around the metal in this complex.

In the crystal structure of **1**, weak interactions are also found between the alkyl hydrogens and non-bridging acetate oxygens from neighboring dimer cation units which result in 1-D supramolecular cationic $\{[Pb(ttpy)(AcO)]_2\}_n^{2n+}$ chains (see figure S1, see online supplemental material at http://dx.doi.org/10.1080/00958972.2014.909930). The 3-D crystal packing pattern in **1** is further afforded by weak interactions between thiocyanate N(4) and the nearest C(12) from the central pyridine of ttpy. Also, weak interactions between thiocyanate S(1) and the pendant aryl groups contribute to the crystal packing.

In the crystal structure, the side pyridine with N(1) is nearly coplanar with the central pyridine ring of ttpy forming an angle of 0.42° between the corresponding mean planes. However, the other side pyridine slightly deviates from coplanarity with the central pyridine ring (the angle between the corresponding mean planes is 8.29°). Also, the pendent tolyl is slightly twisted, forming an angle of 7.32° with the central pyridyl. Such a twisting could arise from $C\text{-}H_{aryl}\cdots S_{thiocyanate}$ and $C\text{–}H_{alkyl}\cdots O_{acetate}$ weak interactions in the crystal packing [see figure 1(b)].

Weak interactions as well as the stereochemically active lone pair of electrons on Pb(II) are responsible for crystal packing of **1** [figure 1(b)]. All ttpy ligands are parallel in the crystal packing, forming a layered packing structure with an intermolecular distance of 4.130 Å exhibiting typical π–π stacking interactions in an offset fashion (slipped face to face) [25–28].

3.3. *Crystal structures of 2 and 3*

Complexes **2** and **3** crystallize in the monoclinic system (space group $P2_1/n$ and $C2/c$, respectively). Selected bond distances and angles are listed in table 2 and hydrogen bonding parameters and weak interaction distances are given in table 3. The molecular structure and crystal packing of **2** and **3** are represented, respectively, in figures 2 and 3. Compared to the previously reported $[Pb(TpyCl)(NO_3)_2]_n$, $[Pb(TpyCl)(ClO_4)_2]_n$ [28], and $\{[Pb(TpyCl)Cl][Pb(TpyCl)Cl_2][PbCl_3]\}_n$ [29] coordination polymers and dinuclear $[Pb(TpyCl)Br_2]_2$ [28], the crystal structure of **2** and **3** show mononuclear [Pb(Clphtpy)(AcO)(ClO_4)] for **2** and [Pb(Clphtpy)$(SCN)_2$] for **3** (figures 2 and 3). In **2**, lead(II) is seven coordinate, chelated by three Clphtpy nitrogens and two acetate oxygens. Also, two perchlorate oxygens are weakly coordinated to Pb (see figure 2 and table 2). In comparison, Pb(II) in **3** is five coordinate, bonded to three nitrogens from Clphtpy and two thiocyanate sulfurs (see figure 3 and table 2).

The Pb–N bond length to the central pyridine nitrogen of Clphtpy (2.505(12) and 2.494(7) Å in **2** and **3**, respectively) is comparable to those found in **1** and previously reported **1A** and **1B** [20(f)]. Also, the measured Pb–N bond distances to the side pyridine groups (2.468(14) and 2.550(13) Å for **2** and 2.466(6) Å for **3**) are in the same range as those found for **1** and commonly reported for similar compounds [20(f), 28, 29]. Compared to values observed for **1** and previously reported **1A** and **1B** [20(f)], the $Pb\text{–}O_{acetate}$ distances in **2** (2.530(11) and 2.80(2) Å) are longer than the terminal $Pb\text{–}O_{acetate}$ bonds and shorter than those observed for bridging acetate oxygens. Weak $Pb\text{–}O_{perchlorate}$ coordination in **2** (3.01(1) and 3.07(1) Å) are comparable with those found for a similar compound reported previously

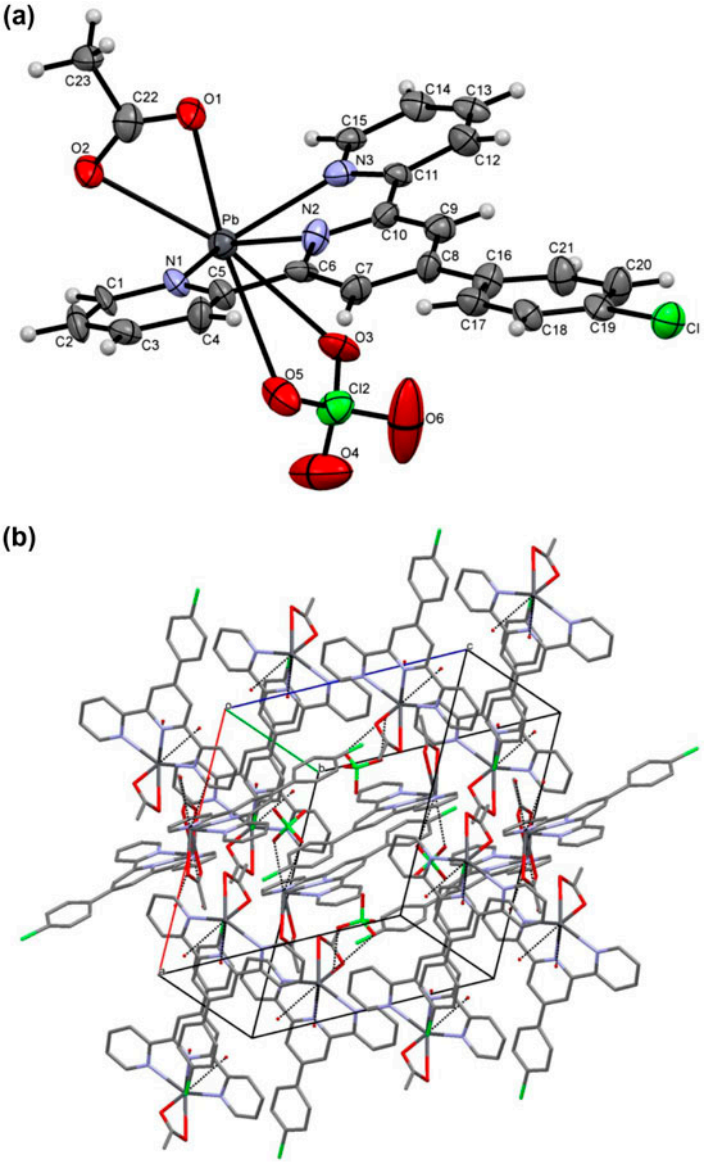

Figure 2. (a) ORTEP view of **2** with the atom numbering scheme. Displacement ellipsoids are shown at the 30% probability level. (b) Packing diagram of **2**.

by our group [28]. Also, the Pb-$S_{thiocyanate}$ bond lengths in **3** (2.951(3) Å) are comparable with the previously reported values for lead(II) thiocyanate complexes with polynitrogen ligands [30].

The measured N–Pb–N angles in the five-membered chelate rings are 65.3(4)° and 64.4 (4)° for **2** which are comparable with the 64.99(12)° found for **3**. The N(1)–Pb–N(3) angle in **2** (128.2(4)°) is similar to that found for **1** and comparable to 130.0(2)° measured for

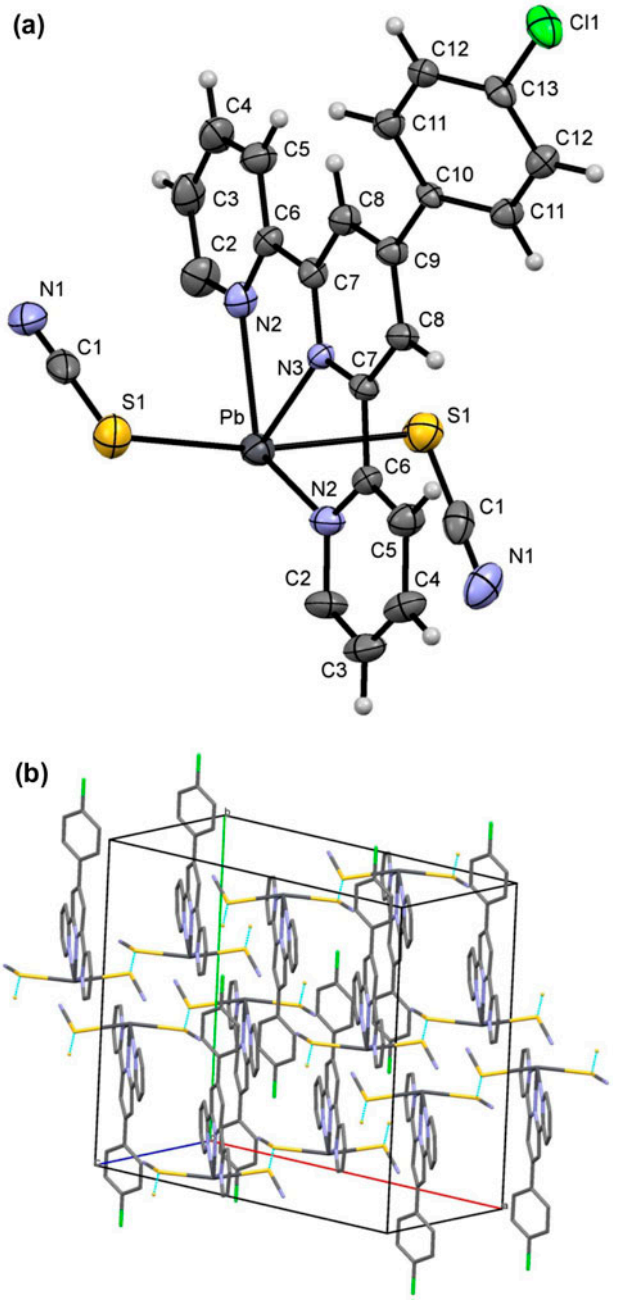

Figure 3. (a) The molecular structure of **3** showing atom numbering scheme, with displacement ellipsoids drawn at the 30% probability level. (b) Packing diagram of **3**.

N(2)–Pb–(N2a) in **3**. The N(1)–Pb–O(1), N(2)–Pb–O(1), and N(3)–Pb–O(1) bond angles in **2** are 86.6(4)°, 84.5(4)°, and 77.2(4)°, respectively. In comparison, the N(2)–Pb–S(1), N(3)–Pb–S(1), and N(2a)–Pb–S(1) angles in **3** are, respectively, 87.17(15)°, 82.20(5)°,

and 86.25(14)°. With perchlorate ion toward the Clphtpy, the related Pb–O bonds in **2** are not perpendicular to the equatorial Pb–N bonds. In the crystal structures of **2** and **3**, the arrangement of donors leaves a wide gap around Pb(II) [figures 2(a) and 3(a)], which presumably is occupied by a 'stereoactive' electron lone pair. Therefore, in solid state, the coordination geometry of Pb(II) is likely to be caused by the geometrical constraints of ligands and by the influence of a stereochemically active electron lone pair in a hybrid orbital on the metal.

The weak interactions and hydrogen bonds in **2** and **3** are represented in table 3. In **2**, intermolecular weak interactions are found between Pb centers and the closest acetate O(1) from the adjacent complex which result in 1-D supramolecular polymers along the crystallographic *b* axis (Pb…O1 distance of 3.32(1) Å and Pb–O1…Pb angle of 162.4(4)°). In the crystal packing, linking of the described supramolecular chains by Pb…$Cl_{Clphtpy}$ weak interactions results in 2-D layers parallel to the (1 0 1) planes (Pb…Cl distance of 3.544(5) Å and C(19)–Cl…Pb angle of 125.2(6)°) (see figure S2 in supplementary material). The corresponding Cl…Pb…O(1), Cl…Pb-N(3), and O(1)…Pb–N(1) angles are 60.5(2)°, 86.8(3)°, and 85.6(4)°, respectively. Also, weak C–$H_{acetate}$…$Cl_{Clphtpy}$ hydrogen bonds are observed in these layers. Versatile weak C–$H_{acetate}$…Pb, $O_{acetate}$…$O_{acetate}$, $C_{Clphtpy}$…O, $C_{Clphtpy}$…$Cl_{Clphtpy}$ supramolecular interactions, and weak C–H…O hydrogen bonds contribute to the 3-D crystal packing of **2** (see table 3).

In the crystal packing of **3**, interconnection of molecular units by weak S…S interactions (Pb–S(1)…S(1) angle of 103.7°) results in formation of supramolecular chains parallel to the *c* axis. By linking the described chains, hydrogen bonding interactions between thiocyanate N and aromatic C–H afford the 3-D crystal packing. The corresponding N(1)…H(5)–C(5) and N(1)…H(12)–C(12) angles are 167.0° and 139.2°, respectively. Also, intermolecular C–H…$C_{aromatic}$ interactions contribute to the crystal packing of **3**.

In the solid state, the central pyridine ring of **2** forms a dihedral angle of 12.07° and 9.10°, respectively, with the plane crossing from C1–N1–C5 and C11–N3–C15, indicating that the three connected pyridyl groups are far from coplanarity. Also, the pendent Clphenyl is twisted forming a dihedral angle of 15.66° with the central pyridyl ring. In comparison, in **3**, the dihedral angles between central pyridine ring and planes crossing the side pyridyl rings are 4.67° with the pendent Clphenyl in this complex rotated to form a dihedral angle of 36.76° with the central pyridyl ring.

3.4. *Biological results*

Micro-organisms can get resistance to antibiotics and their metal complexes through biochemical and morphological modifications [31]. To investigate the effect of counter ions on biological activity, Pb(II), ttpy, and the related **1**, **1A**, and **1B** complexes were tested by MIC method against *K. pneumonia*, *E. coli*, and *S. pyogenes* (see table 4). Biological

Table 4. Results of the antibacterial study of the synthesized compounds (μg mL^{-1}).

	E. coli (−)	*S. pyogenes* (+)	*K. pneumonia* (−)
ttpy	1800	1975	1968
Pb(II) ion	1789	1864	1893
Complex **1**	1640	1790	800
Complex **1a**	600	1835	1844
Complex **1b**	1598	200	1807
Gentamicin	6	8	8

Table 5. IC_{50} of HepG2 cells ($\mu g\,mL^{-1}$).

ttpy	Pb(II) ion	Complex **1**	Complex **1a**	Complex **1b**
1100	37	800	600	900

activity of these complexes can be explained by the presence of lead(II) and on the basis of cell permeability, where lipid membrane around the cell favors the penetration of lipid-soluble materials [32–35].

Very low antibacterial activity is observed for the studied materials, compared to the gentamicin as a standard; however, the activity against different bacteria changes significantly with changing the counter ion. In spite of increased liposolubility of the lead(II) upon chelation by ttpy, increase in the overall volume of complex has a reverse effect and decreases the permeability, perhaps responsible for the observed low activity of these complexes. The three complexes have different actions against bacteria in the range of 20–2000 $\mu g\,mL^{-1}$. Complexes **1**, **1A**, and **1B** exhibit more activity against *K. pneumonia*, *E. coli*, and *S. pyogenes*, respectively. The obtained results indicate the role of counter ions in cell membrane transfer of complexes in different bacteria. Also, controlling the effect of lead(II) lone electron pair activity by counter ions may affect the biological activity of complex.

3.5. *Cytotoxicity results*

To determine the maximum non-toxic concentrations of Pb(II), ttpy, and the synthesized complexes, cytotoxicity test was assessed using MTT assays. The interaction of divalent lead with biological materials has been studied extensively. In this oxidation state, lead binds preferentially to thiol and phosphate in nucleic acids, protein, and cell membranes [36]. According to our results, lead(II) has great cytotoxicity on cultured cells; however, this effect is dramatically decreased for **1**, **1A**, and **1B** (see table 5). While cell membrane transfer of the complexes could be affected by the counter ion, the difference of inner and outer sphere coordination is obvious in the results where direct bonding of iodide to Pb in **1B** more effectively decreases the cytotoxicity of Pb(II). Engagement of Pb lone pair of electrons by iodide, reducing their activity is, possibly, the reason of such behavior in **1B**. This procedure has promising results to find new chelating agents which can be used to remove lead after ingestion.

4. Conclusion

In this work, we report the synthesis and characterization of three new complexes, $\{[Pb(ttpy)(\mu\text{-}AcO)]_2\}(SCN)_2$ (**1**), $[Pb(Clphtpy)(AcO)(ClO_4)]$ (**2**), and $[Pb(Clphtpy)(SCN)_2]$ (**3**) (ttpy = 4′-tolyl-2,2′:6′,2″-terpyridine and Clphtpy = 4′-chlorophenyl-2,2′:6′,2″-terpyridine). Despite coordination ability of thiocyanate group, in the solid state, coordination of lead by acetate is preferred to afford the binuclear $\{[Pb(ttpy)(\mu\text{-}AcO)]_2\}^{2+}$. However, thiocyanates still exist to neutralize the crystal lattice. Compared to the previously reported $\{[Pb(ttpy)(\mu\text{-}AcO)]_2\}(PF_6)_2$ (**1A**) and $\{[Pb(ttpy)(\mu\text{-}AcO)I]_2\}$ (**1B**) [20(f)], the variations observed in **1** for the unit cell dimensions, cell volumes, coordination bond lengths, and dihedral angles between side pyridine rings are directly related to the coordination ability of the counter ion and also depend on the inter- and intramolecular weak interactions [37].

In contrast to **1**, by replacing the methyl by chlorine on the pendent phenyl group in ttpy, mononuclear complexes **2** and **3** are formed. Comparable to that found for **1**, coordination of one acetate to Pb(II) is still preferred in **2** and the second acetate is replaced by one perchlorate. However, both acetates are replaced by thiocyanate to form mononuclear complex [Pb(Clphtpy)$(SCN)_2$] (**3**). Coordination geometry of the lead(II) in the complexes is hemidirected.

Although low antibacterial activities were observed for **1**, **1A**, and **1B** (due to the low permeability of cell membrane to the complexes), the activities are observed to change significantly by changing the counter anion for different bacterium. Moreover, cytotoxicity results indicated that, compared to lead(II), the cytotoxicity to human liver carcinoma (HepG2) cells is dramatically decreased for **1**, **1A**, and **1B**. The cytotoxicity of lead(II) was controlled by ttpy complexation. Moreover, further controlling the activity of lone electron pair on Pb(II) by coordinating counter anions, better results were observed.

Supplementary material

CCDC numbers of 914472, 936288, and 957927 for {[Pb(ttpy)(μ-AcO)]$_2$}$(SCN)_2$ (**1**), [Pb(Clphtpy)(AcO)(ClO_4)] (**2**), and [Pb(Clphtpy)$(SCN)_2$] (**3**), respectively, contain the supplementary crystallographic data for this article. These data can be obtained free of charge via http://www.ccdc.cam.ac.uk/conts/retrieving.html or from the Cambridge Crystallographic Data Center, 12 Union Road, Cambridge CB2 1EZ, UK; Fax: (+44) 1123 336 033; or E-mail: deposit@ccdc.cam.ac.uk. Figures S1 and S2 represents the supramolecular structures in the crystal packing of complexes **1** and **2**, respectively.

Acknowledgements

Support of this investigation by the Payame Noor University, Iran and Atatürk University, Erzurum, Turkey is gratefully acknowledged.

References

[1] N.R. Lien, M.A. Timmons, G.J.H. Belkin, J.R. Holst, M.L. Janzen, R. Kanthasamy, W. Lin, A. Mubayi, M.I. Perring, L.M. Rupert, A. Saha, N.J. Schoenfeldt, A.N. Sokolov, J.R. Telford. *Inorg. Chim. Acta*, **358**, 1284 (2005).
[2] H. Li, S.P. Webb, J. Ivanic, J.H. Jensen. *J. Am. Chem. Soc.*, **126**, 8010 (2004).
[3] A.C. Larsson, A.V. Ivanov, K.J. Pike, W. Forsling, O.N. Antzutkin. *J. Mag. Res.*, **177**, 56 (2005).
[4] W. Shi, X.Y. Chen, B. Zhao, A. Yu, H.B. Song, P. Cheng, H.G. Wang, D.Z. Liao, S.P. Yan. *Inorg. Chem.*, **45**, 3949 (2006).
[5] A. Morsali, A.R. Mahjoub. *Inorg. Chem. Commun.*, **7**, 915 (2004).
[6] J.S. Seo, D. Whang, H. Lee, S.I. Jun, J. Oh, Y.J. Jeon, K. Kim. *Nature*, **404**, 982 (2000).
[7] S. Mondal, M. Mukherjee, S. Chakraborty, A.K. Mukherjee. *Cryst. Growth Des.*, **6**, 940 (2006).
[8] E. Alessio, Y. Xu, S. Cauci, G. Mestroni, F. Quadrifoglio, P. Viglino, L.G. Marzilli. *J. Am. Chem. Soc.*, **111**, 7068 (1989).
[9] A.S. Gaballa, M.S. Asker, A.S. Barakat, S.M. Teleb. *Spectrochim. Acta, Part A*, **67**, 114 (2007).
[10] J.M. Ratcliffe. *Lead in Man and Environment*, Wiley, New York (1981).
[11] (a) L. Shimoni-Livny, J.P. Glusker, C.W. Bock. *Inorg. Chem.*, **37**, 1853 (1998); (b) R.D. Hancock, M.S. Shaikjee, S.M. Dobson, J.C.A. Boeyens. *Inorg. Chim. Acta*, **154**, 229 (1998).
[12] A. Morsali. *J. Coord. Chem.*, **59**, 1015 (2006).
[13] V. Balzani, F. Scandola. *Supramolecular Chemistry*, Harwood, Chichester (1991).

[14] V. Balzani, A. Juris, M. Venturi, S. Campagna, S. Serroni. *Chem. Rev.*, **96**, 759 (1996).
[15] C.G. Wu, T. Bein. *Chem. Commun.*, **8**, 925 (1996).
[16] F. Barigelletti, L. Flamigni, J.P. Collin, J.P. Sauvage. *Chem. Commun.*, **4**, 333 (1997).
[17] H. Oshio, H. Spiering, V. Ksenofontov, F. Renz, P. Gütlich. *Inorg. Chem.*, **40**, 1143 (2001).
[18] J.F. Michalec, S.A. Bejune, D.G. Cuttell, G.C. Summerton, J.A. Gertenbach, J.S. Field, R.J. Haines, D.R. McMillin. *Inorg. Chem.*, **40**, 2193 (2001).
[19] S.B. Jones, L.J. Tiffany, K. Garmestani, O.A. Gansow, R.W. Kozak. *Nucl. Med. Biol.*, **23**, 105 (1996).
[20] (a) L.A. Saghatforoush, L. Valencia, F. Chalabian, S. Ghammamy. *Bioinorg. Chem. Appl.*, **2001**, 1 (2001); (b) L.A. Saghatforoush, L. Valencia, F. Chalabian, S. Ghammamy, L.Z. Khaledi. *J. Coord. Chem.*, **64**, 3311 (2011); (c) L.A. Saghatforoush, S.G. Telfer, F. Chalabian, R. Mehdizadeh, R. Golbedaghi, G.H. Shahverdizadeh. *J. Coord. Chem.*, **64**, 2186 (2011); (d) L.A. Saghatforoush, L. Valencia, F. Chalabian, S. Ghammamy, F. Katouzian. *J. Chem. Sci.*, **124**, 577 (2012); (e) L.A. Saghatforoush, K. Adil, M. Hasanzadeh, A. Aminkhani, S. Safarinezhad. *Acta Chim. Slov.*, **59**, 322 (2012); (f) L.A. Saghatforoush, K. Adil, E. Sahin, S. Babaei, S.J. Musevi. *J. Coord. Chem.*, **64**, 4421 (2011).
[21] L.J. Farrugia. *CrystalClear™ Software*, Rigaku Inc., Texas, USA (2005).
[22] G.M. Sheldrick. *SHELX-97 Program Package, SHELXS-97 and SHELXL-97*, University of Göttingen, Göttingen, Germany (1997).
[23] M.R. Malik, V. Vasylyeva, K. Merz, N. Metzler-Nolte, M. Saleem, S. Ali, A.A. Isab, K.S. Munawar, S. Ahmad. *Inorg. Chim. Acta*, **376**, 207 (2011).
[24] (a) K. Nakamoto. *Infrared and Raman Spectra of Inorganic and Coordination Compounds, Part B, Applications in Coordination, Organometallic, and Bioinorganic Chemistry*, 6th Edn, p. 121, Wiley, New Jersey, NJ (2009); (b) D.H. Williams, I. Fleming. *Spectroscopic Methods in Organic Chemistry*, 4th Edn, McGraw Hill, London (1989).
[25] J.E. Beves, P. Chwalisz, E.C. Constable, C.E. Housecroft, M. Neuburger, S. Schaffner, J.A. Zampese. *Inorg. Chem. Commun.*, **11**, 1009 (2008).
[26] A.F. Williams, C. Floriani, A.E. Merbach. *Perspectives in Coordination Chemistry*, p. 129, VCH, Basel (1992).
[27] R.D. Hancock, M.S. Shaikjee, S.M. Dobson, J.C.A. Boeyens. *Inorg. Chim. Acta*, **154**, 229 (1988).
[28] F. Marandi, L. Saghatforoush, I. Pantenburg, G. Meyer. *J. Mol. Struct.*, **938**, 277 (2009).
[29] L. Saghatforoush, F. Marandi, I. Pantenburg, G. Meyer. *Z. Anorg. Allg. Chem.*, **635**, 1523 (2009).
[30] D.L. Reger, T.D. Wright, M.D. Smith, A.L. Rheingold, S. Kassel, T. Concolino, B. Rhagitan. *Polyhedron*, **21**, 1795 (2002).
[31] P. Pyykko. *Chem. Rev.*, **88**, 563 (1988).
[32] S. Tardito, A. Barilli, I. Bassanetti, M. Tegoni, O. Bussolati, R. Franchi-Gazzola, C. Mucchino, L. Marchiò. *J. Med. Chem.*, **55**, 10448 (2012).
[33] S. Tardito, I. Bassanetti, C. Bignardi, L. Elviri, M. Tegoni, C. Mucchino, O. Bussolati, R. Franchi-Gazzola, L. Marchiò. *J. Am. Chem. Soc.*, **133**, 6235 (2011).
[34] T. Mosmann. *J. Immunol. Methods*, **65**, 55 (1983).
[35] P.B. Tchounwou, B.A. Wilson, A.B. Ishaque, J. Schneider. *Mol. Cell. Biochem.*, **222**, 49 (2001).
[36] T.S. Cruz, P.A. Faria, D.P. Santana, J.C. Ferreira, V. Oliveira, O.R. Nascimento, G. Cerchiaro, C. Curti, I.L. Nantes, T. Rodrigues. *Biochem. Pharm.*, **80**, 1284 (2010).
[37] M.M. Ibrahim, A.M.M. Ramadan, G.A.M. Mersal, S.A. El-Shazly. *J. Mol. Struct.*, **998**, 1 (2011).